Pitting Resistance of Worm Gears: Advanced Model for Contact Pattern of Any Size, Position, Flank Type

Prof. Dr.-Ing. K. Stahl, Prof. Dr.-Ing. B.-R. Höhn,
Dr.-Ing. J. Hermes, Dipl.-Ing. A. Monz

An experimental and theoretical analysis of worm gear sets with contact patterns of differing sizes, position and flank type for new approaches to calculation of pitting resistance.

Nomenclature

a	Center distance	(mm)
l_{eff}	Effective width of line contact	(mm)
n_1	Input rotational speed	(min^{-1})
u	Gear ratio	(-)
E'	Reduced e–module	(N/mm^2)
F_N	Normal force	(N)
K	Stribeck rolling pressure	(N/mm^2)
L_{hI}	Pit lifetime in Phase I	(h)
N_{LI}	Stress reversals in Phase I	(-)
ρ_E	Equivalent radius of curvature	(mm)
σ_H	Hertzian stress	(N/mm^2)
σ_{Hm}	Mean Hertzian stress	(N/mm^2)

Introduction

In highly loaded, steel-bronze worm gear sets, their maximum capacity is determined primarily by the types of damage incurred; i.e., "tooth breakage" and "pitting." In practice, larger-size worm gears are those with a center distance of more than 200 mm. Unlike a steel-steel or steel-cast iron material combination, pitting damage to a bronze worm wheel does not necessarily lead to teeth failure. Rather, the pitting area may in fact decrease due to the gradual, abrasive wear of the affected surface. Though pitting initially reduces the meshing area of both worm and worm wheel, it will induce noise and reduce gear set efficiency. Therefore precise knowledge of the pitting lifetime of large, high-efficiency worm gear sets is an important design criterion.

To facilitate actual assembly of a worm gear, convex—i.e., shell-shaped—contact patterns are typically produced—although smaller when compared to a completely formed contact pattern. Thus the initial position of the contact pattern between worm and worm wheel is more easily determined and optimally adjusted. Most often, the transmissions are immediately exposed to system operating conditions and rarely subjected to run-in. Because the abrasive wear on the worm wheel of large-size gear sets is minor, no complete contact pattern is formed for most of its lifetime. And, as no mathematical proof determining early pitting resistance of worm gear sets caused by insufficient contact pattern has yet to be documented, providing such mathematical proof has been the main motivation for this research.

The State of the Art

Calculation of pitting lifetime is primarily based on the analysis of Rank (Ref. 12), which is contained in the calculation method DIN 3996 (Ref. 4). Calculation of pitting lifetime is recommended according to (Ref. 4) if the calculated pitting safety is $S_H < 2.0$. This is usually the case—especially for large worm gear sets with typical low wear intensity. Rank (Ref. 12) subjects his test gear sets to a long run-in with reduced load and achieves a full contact pattern between worm and worm wheel without prior deterioration of the flanks. Current technology requires therefore a completely formed contact pattern between worm and worm wheel in the calculation.

Pitting is generally ascribed to a surface spalling of the material due to repeated overstepping of the allowed fatigue limit and the material's so-called "rolling strength." Pitting occurs on the weaker of the two rolling contact partners—typically the worm wheel bronze. Rank (Ref. 12) explains this procedure by the changing mechanical stresses in the claimed surface areas in the tribological system tooth contact. The local Hertzian stresses in the tooth contact between worm and worm wheel are not constant and change continuously. If the yield stress is exceeded, they begin with the first operating phase and through the adaption of the worm wheel flank to the worm flank by abrasive wear and a local yielding of the worm wheel material. This means that the appearance of initial pitting damage can always be explained by the overload of a discrete flank section. Depending on the present rolling strength of the worm wheel material, these loads are able to bear a specific number of stress reversals until the flank area quarries out in the form of pitting. According to (Ref. 12), pitting and its associated wear intensity can be subdivided into three characteristic sections. The pitting area described by the pitting parameter A_{P10} on the worm wheel can be used to define these sections. A_{P10} represents the average pitting area of the most damaged teeth in percentage; the value is deduced from the overlap and is approximately 10% of the worm wheel teeth. The lifecycle begins with Phase I—i.e., the stage of no pitting and low wear intensity. At this point there is no damage to the wheel flanks; the gear set, with its still fragmentary contact pattern, is run-in during this phase; the contact patterns grows; the cutting marks and roughness peaks of flanks are straightened; and the resulting peaks of Hertzian stress are partially reduced. By local exceeding of the

This article originally appeared (in German) in the April 2012 issue of Antriebstechnik.

rolling strength, surface cracks appear that may cause pitting. The end of Phase I is defined with $A_{P10} = 2\%$.

In Phase II—during which pitting growth occurs—in linear terms the pitting area enlarges approximately to a maximum-area A_{P10max}. A maximum-value A_{P10max} of 60–80% is usually benign and trouble-free operation of the gear set results.

However, when the maximum pitting area is reached, wear intensity increases, leading to Phase III—i.e., decreasing pitting and comparably high wear. The incipient sliding wear—clearly exacerbated due to the significantly reduced meshing area—in turn reduces the pitting area. Upon further operation, end-of-teeth lifetime is eventually reached due to collateral damage such as wear limit, tooth breakage or impermissible, high-transmission errors and induced vibrations and noise.

Rank (Ref. 12) analyzes the influencing variables of pitting and its proliferation and devises a wear-based approach for predicting the pitting lifetime of the three pitting phases described above. He affirms the reports of Niemann (Ref. 9), stating that the essential influence at play in the pitting of worm gear drives is Hertzian stress in tooth contact and, thus, premature pitting damage begins with growing Hertzian stresses. Experiments examining variation of the sliding speed of the teeth show that the beginning of pitting is barely influenced by such sliding speed and concerns can be dismissed for the lifetime of Phase I. The speed of the pitting increases in Phase II due to low sliding speed. From these coherences (Ref. 12) derive approximate formulas for lifetimes in the three pitting phases relevant to mean sliding speed and mean Hertzian stress. Here it is assumed that a finished run-in of the worm wheel flank leads to a consistent distribution of Hertzian stress—an approach based on Predki (Ref. 11), who derived the physical parameter p^* from calculation of the pressing distribution in teeth contact—and assuming that Hertzian stress along the lines of contact—which are in contact at the same time—are constant. Conversely, Bouché (Ref. 2) detected an irregular pressure distribution based on an approach of a wearing of the friction lining for a run-in worm gear set. He compares the results with the experiments of Böhmer (Ref. 1). In doing so he discovered a good correlation of the maximum values for Hertzian stress and pitting location; Wilkesmann (Ref. 16) calculated similar results for pressure distribution. And, Octrue (Ref. 10) and Hermes (Ref. 5) affirm this correlation based upon their own calculation approaches. Rank (Ref. 12) diversifies further the location of the primary contact pattern between worm and worm wheel. As a result, pitting location depends essentially on the location of the primary contact pattern; i.e.—the time until initial pitting and its subsequent spread to a maximum-area-of-damage the size of the primary contact pattern. Through the work of Lutz (Ref. 8), Weisel (Ref. 15) and Sievers (Ref. 13), it is possible to calculate pressure distribution for incomplete contact patterns. Weisel (Ref. 15) conducted numerous experimental inquiries and formulated an approach for calculating development of contact pattern, wear-carrying capacity and efficiency of worm gear sets with complete contact pattern during operation. He (Ref. 15) compares the calculated results to Rank's (Ref. 12) global calculation of pitting lifetime and determines that pitting lifetime—which was achieved in the examination—is much lower than once thought.

And yet, an all-embracing approach for contact patterns of any size, position and Flank-Type—offering a reliable prediction for the onset and location of pitting—does not yet exist.

Such an approach is introduced in the following.

Test Stand Operations

This analysis presents a method for predicting the location and pitting lifetime of worm gears of all sizes, positions and Flank-Types. Accordingly, a battery of Phase 1 tests were conducted on worm gear sets with knowingly uncompleted contact patterns and then evaluated; the results were compared to the new method. The initial contact patterns of the worm gears are comparable in position and size to those typically found in industrial applications.

Test conditions. The operations were carried out with cylindrical worm gear sets with Flank-Type I and C with a center distance between 100–315 mm and a gear ratio of 6.6–24.5. The tests with a center distance of $a = 170$ mm, $a = 180$ mm and $a = 250$ mm were run on Siemens test rigs. The tests with a center distance of $a = 315$ mm were conducted at FZG (*Forschungsstelle für Zahnräder und Getriebebau—Prof. Dr.-Ing. K. Stahl—TU München, Garching).* The re-evaluation of testing conducted by (Refs. 12 and 15)—which should serve to validate the new approach for completed contact patterns—was also done at FZG. Testing with the reference standard teeth—(Ref. 4)—and with reduced contact pattern—was also done at FZG. Additional research of pitting and pitting growth was conducted by Jacek (Ref. 7) on worm gear sets at LMGK (*Lehrstuhl für Maschinenelemente, Getriebe und Kraftfahrzeuge—Prof. Dr.-Ing. W. Predki—Ruhr-Universität Bochum, Bochum*). These, too, were used for validation of the new calculation approach. Thus the experimental matrix covered the scope (Ref.4) for concave-convex and convex-convex wheel sets and expanded it for greater center distances ($a >$ 250 mm).

Case-hardened worms made of 16MnCr5 and gear rims made of CuSn12Ni2-C-GZ were used, with the required bronze meeting the high quality standards of the "worm gears research group" of FVA that were developed and optimized in the framework of numerous research projects. Polyglycols (viscosity classes ISO VG 220 and 460) were used as lubricants. The gear sets were operated with differing input rotational speeds and with comparatively high output torques within their catalogue nominal torque. The mean Hertzian stresses (Ref. 13) were in the range of $\sigma_{Hm} = 344$ and 496 N/mm^2. Table 1 addresses the entire experimental matrix—i.e., the essential specifications of load and teeth for the analyzed gear sets, as well as contact pattern positions and sizes.

Evaluation of the test. Testing was done at continuous output torque and continuous input rotational speed. Rotational speeds and torques at the input and output shaft were measured continuously throughout the test sequence. In periodic time steps the flanks of the wheels were photographically documented. Wear revealed by testing with a center distance of $a = 315$ mm

No. [-]	Size a [mm]	Gear Ratio z_2 / z_1 [-]	Flank Type [-]	Input Speed n_1 [min^{-1}]	Output Torque T_2 [Nm]	Mean Hertzian Stress σ_{Hm} [N / mm²]	Contact Pattern [-] Inlet Side Outlet Side
1	100	41 / 2	I	1500	860	451	
2	170	33 / 5	C	1500	1755	344	
3	180	49 / 2	C	1500	2920	374	
4	250	55 / 2	C	870	9000	410	
5	250	55 / 2	C	870	9000	496	
6	315	37 / 2	C	1500	15750	447	
7	315	37 / 2	C	1500	15750	422	
8	315	41 / 2	I	1500	15750	420	
9	315	41 / 2	I	1500	15750	395	

Table 1 Test gear sets data.

was detected by incremental encoders in periodic time steps. The evaluation of the tests carried out here—(Refs. 7, 12 and 15)—was based on the information set out there and on the test documentation.

The values of the mean Hertzian stresses allowing for an uncompleted contact pattern at the beginning were calculated by the program *ZSB* (Ref. 14) and modified (Ref. 13). On that basis the calculation of pitting lifetime in Phase I is in line with the proven method (Ref. 4), based on the parameter for mean Hertzian stress p^* (Ref. 11).

The distribution of pressure in the meshing area of the worm and worm wheel was calculated by the program *SNETRA* (Refs. 8 and 15). Accordingly, the maximum values of the Hertzian stresses in the entire meshing area for the gear set without run-in were examined. The results were used to compare the simulation with the documented location of pitting during the test runs.

Test Results

Development of contact pattern and wear. The worm gear sets for the test runs were designed and manufactured to show the earliest contact patterns, with typical size and position. Because of the low wear of the analyzed center distances, the contact pattern grows very slowly during run-in and pitting begins. Figure 1 shows an example of the characteristic development of contact pattern and of the wear of $a = 315$ mm worm wheel with Flank-Type C. The figure also shows the expected development of contact pattern and the pressure distribution over lifetime, which is determined by the program (Ref. 15).

Further, the worm wheel has an almost-constant wear intensity of about 12 µm-per-one-million-load cycles after approximately 0.6 million load cycles. Considerable run-in wear—typical for worm gear sets of smaller center distances—does not exist at that point. The smoothing of surfaces—by virtue of reducing the roughness peaks and adaption of the worm wheel flanks to the geometry of the worm—are finished as completely as possible. Weisel (Ref. 15) detects similar values for the abrasive wear on worm wheels with Flank-Type I of similar size, total sliding speed, lubrication and Hertzian stress.

In Test 6, 106 µm flank abrasion is necessary for attaining a complete contact pattern. Based on the wear rate referred to above, this complies with about 6 million load cycles; but there is already a pitting area of $A_{P10} = 2\%$ on the flank after 2 million load cycles.

A calculation using the approach for completed contact pattern (Ref. 12) is not possible because no completed contact pattern exists and the occurring Hertzian stresses are considered too low. This approach therefore requires an overly long calculated pitting lifetime of about 6 million load cycles. As such, this calculation—as it currently exists—cannot be used for this typical, practical case.

Location of pitting. Following are statements made about the location of pitting on worm wheel flanks using calculated pressure distribution (Ref. 15). Such statements can often be found in the existing literature, indicating the beginning of pitting on the outlet side of the worm wheel and then growing in the direction of the inlet side during further operation. This statement is based—more on observation and less on the fact—on the premise that maximum pressure can be localized on the outlet side of the chosen gear set. To describe clearly the direct correlation between location of maximum Hertzian stress and location of initial pitting, the distribution of Hertzian stress that was calculated (Ref. 15) was systematically evaluated and compared to the test results in this study.

The local Hertzian stress σ_H in the teeth contact is calculated according to Equation 1, based on Stribeck rolling pressure K and the reduced module of elasticity of the material combination of worm and worm wheel E'.

$$\sigma_H = \sqrt{K \cdot \frac{E'}{\pi}} \tag{1}$$

For calculating the pressure distribution of the entire meshing area, the worm and worm wheel were divided into numerous pieces along a contact line; for these pieces the local Hertzian stresses were calculated. Equation 2 shows that the Stribeck rolling pressure K behaves inversely proportional to the equivalent radius of curvature if the normal force F_N on the considered section of the contact line and the length of the bearing section l_{eff} are the same; Hertzian stress σ_H behaves accordingly. A large equivalent radius of curvature thus leads to a low Hertzian stress, and vice versa.

$$K = \frac{F_N}{2 \cdot \rho_E \cdot l_{eff}} \tag{2}$$

If the contact pattern of a worm gear is reduced, the line load F_N increases in approximate measure for the entire contact area. Due to the slightly different—yet equivalent—radius of curvature of nearby flank points, the local Hertzian stress increases proportionally in accordance with Equations 1 and 2. If the contact pattern is large enough, it is allowed to determine the location of pitting for

reduced contact patterns between worm and worm wheel, and also from the pressure distribution of a completed contact pattern. Figure 2 shows the equivalent radius of curvature (Ref. 15) of four different worm gearings with Flank-Type I and a center distance of $a = 100$ mm over a gear ratio range of 8 and 50. The lower part of Figure 2 shows the distribution of Hertzian stress along the worm wheel flank (Ref. 15). In that the stiffness of the worm wheel is already considered, i.e.—along the contact line—a variable line load is calculated that is dependent on the mesh position.

It is very clear that the location of maximum Hertzian stress is essentially determined by the location of the minimum equivalent radius of curvature; this accordance is described in (Refs. 5, 9, 10 and 16) as well. It is also clear that the equivalent radiuses of curvature on the whole flank show significantly different values, and yet are very similar in neighboring areas. It is also readily apparent that the ratios vary in the position of the minimum-equivalent radius of curvature, and in the position of the maximum-occurring Hertzian stress.

It is seen that the local equivalent radius of curvature influences the pitting location. The equivalent radiuses of curvature are basically determined by Flank-Type, gear ratio and profile shift. Figure 3 shows the comparison of pitting for Flank-Type C and I with the calculated development of the contact lines and of the pressure distribution of Tests 7 and 8; both gearings have comparable gear ratios. This comparison makes clear the fact that the pitting occurs in the tooth root with Flank-Type C and, with Flank-Type I, on the outlet side.

The pitting locations in the tests corresponded very well with the calculated (per *SNETRA,* Refs. 8 and 15) location of the maximum Hertzian stress. Depending upon Flank-Type and gear ratio, this can be positioned in various places. For this reason, assumptions regarding pitting location can be confirmed both empirically and arithmetically and, therefore, be pre-calculated. Based on this coherence, flanks of worm and worm wheels can be optimized systematically in consideration of the pressure distribution.

Pitting growth on worm wheel flanks. Figure 4 shows extremely advanced pitting in lifetime Phases I and II on four uniformly distributed teeth around the circumference of a test gearing of size $a = 170$ mm with Flank-Type C (Test 2, Table 1).

Thus, pitting occurs almost simultaneously on all teeth of the worm wheel. In addition, the pitting location is almost the same for all teeth. In Figure 4 the location of pitting is illustrated by horizontal lines. Pitting begins at the place of maximum Hertzian stress and continues growing from there towards the inlet side. If the reason for the pitting was defective areas in the bronze, its location would to some degree be statistically distributed around the circumference of the worm wheel. Also, the pitting growth in the affected areas of the tooth flanks is very consistent; i.e.—no tooth of the worm wheel has an appreciably larger pitting area than the other teeth. This behavior was evidenced in every reviewed gearing test for this study. A high-quality worm wheel bronze with few defective areas and homogeneous microstructure—and gearing with fractional tooth deviations corresponding to gear tooth quality 7 according to DIN 3974 (Ref. 3) or better—are preconditions for such evenly distributed pitting.

Point-of-time of pitting (end of Phase I). As expected, premature pitting occurred on the worm wheel flanks during all test runs. This was due to the reduced contact patterns; a complete contact pattern was not built in any test run.

It was also shown that the pitting location coincides with the pre-calculated maximum Hertzian stress in the engagement region of the gearing. The current benchmark requires a complete contact pattern and, therefore, cannot address the influence of a reduced-size contact pattern on the existing Hertzian stress. If the contact pattern decreases, the minimum/maximum values of the flank-occurring Hertzian stress converge due to the equivalent radiuses of curvature (Eq. 1). In the extreme case of a punctiform contact pattern—e.g., crossed helical gears—the maximum and mean Hertzian stress would be the same. It is therefore permissible to use the mean Hertzian stress—calculated for incomplete contact patterns—as significant load under the simplifications (Ref. 11).

Figure 5 shows the Phase I lifetime of all conducted tests, depending on the calculated mean Hertzian stress and the appropriate 15% scatter band in the form of a Woehler diagram. The calculation of the mean Hertzian stress is conducted (Ref. 13) with reference to the contact patterns shown in Table 1. Further, the results of experiments (Refs. 7 and 12) are illustrat-

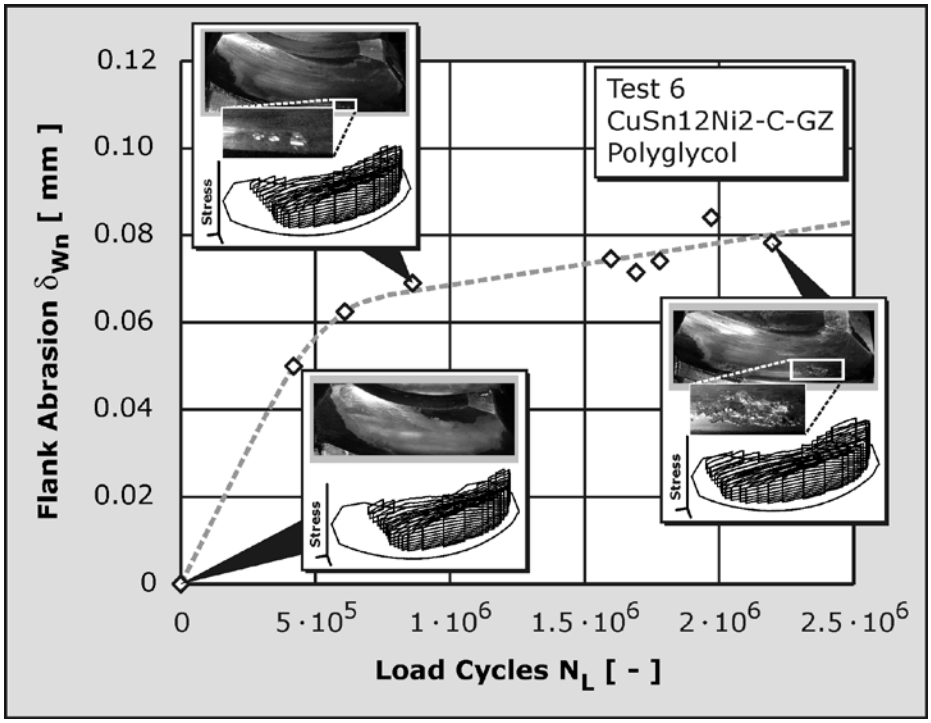

Figure 1 Wear and development of contact pattern: Test 6.

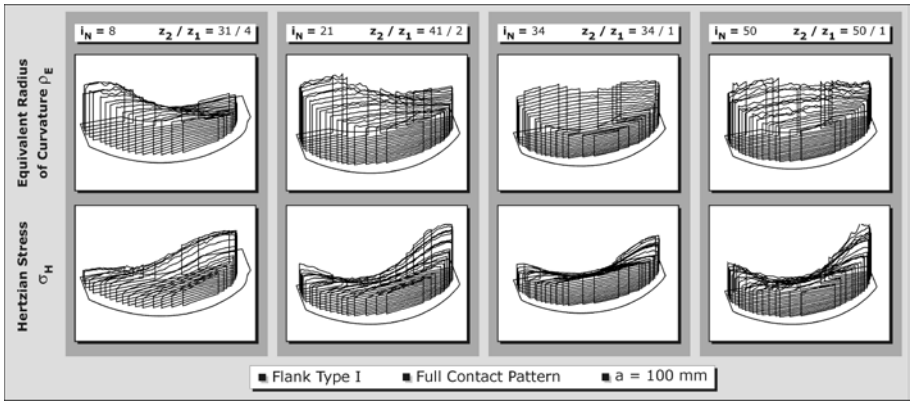

Figure 2 Equivalent radiuses of curvature for worm gear sets with different gear ratios.

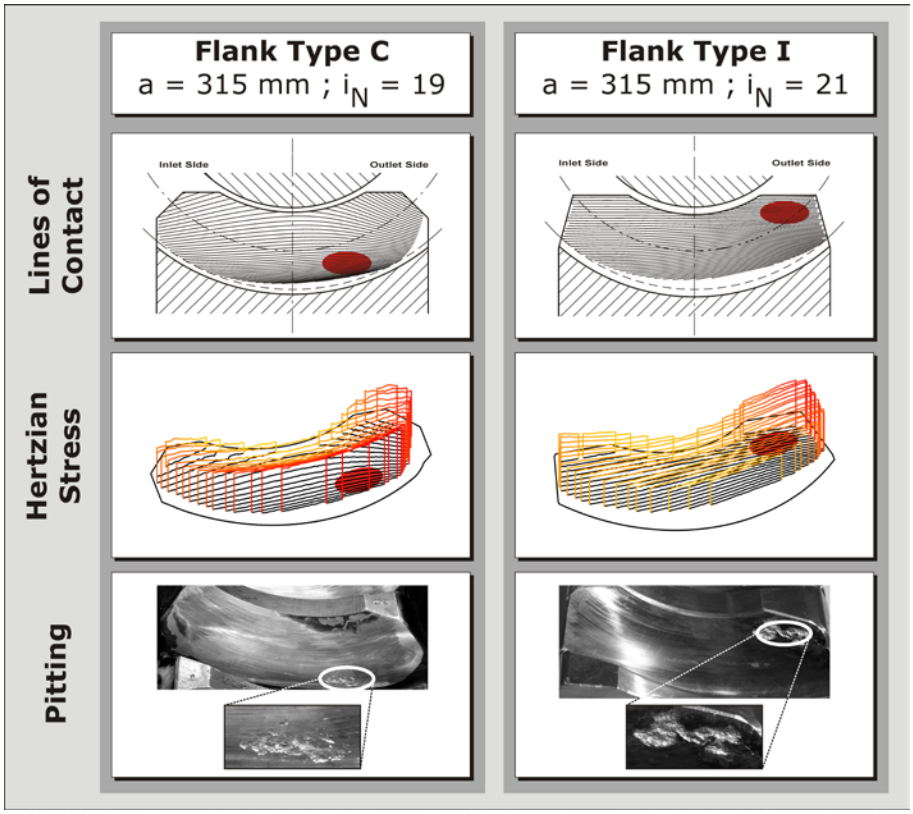

Figure 3 Location of pitting dependent upon flank type: Tests 7 and 8.

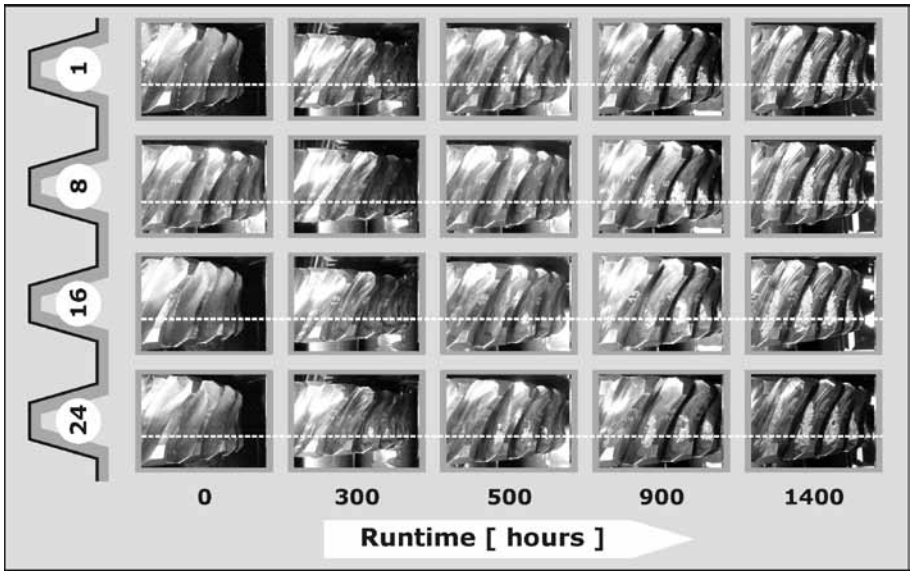

Figure 4 Pitting on test wheel: A = 170 mm; Flank Type C, z_2/z_1 = 33/5 (Test 2, per Fig. 1).

ed based on the mean Hertzian stress for a complete contact pattern.

An upper limit for the mean Hertzian stress 500 N/mm^2 was assessed. Beyond this value, deformations under load (Ref. 12) are no longer purely elastic and the adaptability of a direct coherence of pressure and stress reversals cannot be confirmed. Thus, flowing effects arise in the material of the worm wheel that provide—through redistribution of the worm wheel material—a partial reduction of local Hertzian stress. However, because all gear sets are operated with their catalogue-nominal torque, and stay so far below the limit of pressure, the method covers the most commonly used worm gear sets. The newly established function shows very good dependency of the reachable stress reversals in lifetime Phase I on the mean Hertzian stress. Furthermore, it became apparent that this method delivers reliable results for complete contact patterns as well.

Therefore, the sliding speeds in the contact—which occur differently during live testing (Table 1)—have in Phase I no measurable influence on the initiation point of pitting. This confirms similar results of (Ref. 12).

Equation 3 describes the functional coherence between stress reversals N_{LI}—until reaching the $A_{P10} = 2\%$ criterion—and the mean Hertzian stress σ_{Hm} calculated (Ref. 13) for worm wheel bronze CuSn12Ni2-C-GZ lubricated with polyglycol.

$$N_{LI} = \left(\frac{2650}{\sigma_{Hm}}\right)^{7.8} \text{für } \sigma_{Hm} \leq 500 \frac{N}{mm^2} \qquad (3)$$

According to Equation 4, the onset of pitting L_{hl} is prevented with the gear ratio u and input rotational speed n_1 calculation.

$$N_{LI} = \frac{N_{LI} \cdot u}{n_1 \cdot 60} \qquad (4)$$

Conclusions

In practice, worm gears evidence a reduced contact pattern at the outset. The local high Hertzian stress—combined with the low wear rate of larger center distances—leads quickly to localized pitting. The until-now-accepted calculation for pitting lifetime, however, requires a completely run-in contact pattern between worm and worm wheel.

On the basis of experimental and theoretical investigations of the tooth contact of worm gearings, a new method for calculating pitting lifetime is presented,

which also can be used on incomplete contact patterns. It enables—*for the first time*—the calculation of practical, incomplete contact patterns as they apply to pitting lifetime and provides enhanced optimization of worm gears.

The Hertzian stress in the tooth contact between worm and worm wheel is assessed as significant load. This new method can also be applied for complete contact patterns. Accordingly, the results of previous research in this field with complete contact patterns can be comprehended and calculated as well.

In the above-described calculation method, existing calculation approaches for the location of pitting were applied, systematically verified and approved by virtue of experimental results. It is now therefore possible—also for the first time—to reliably predict the location of pitting of worm gear sets with contact patterns of any size, position and Flank-Type with a broad area of validation. Indeed, optimal load distributions of a worm gear set can now be directly determined and load-carrying capacity enhanced.

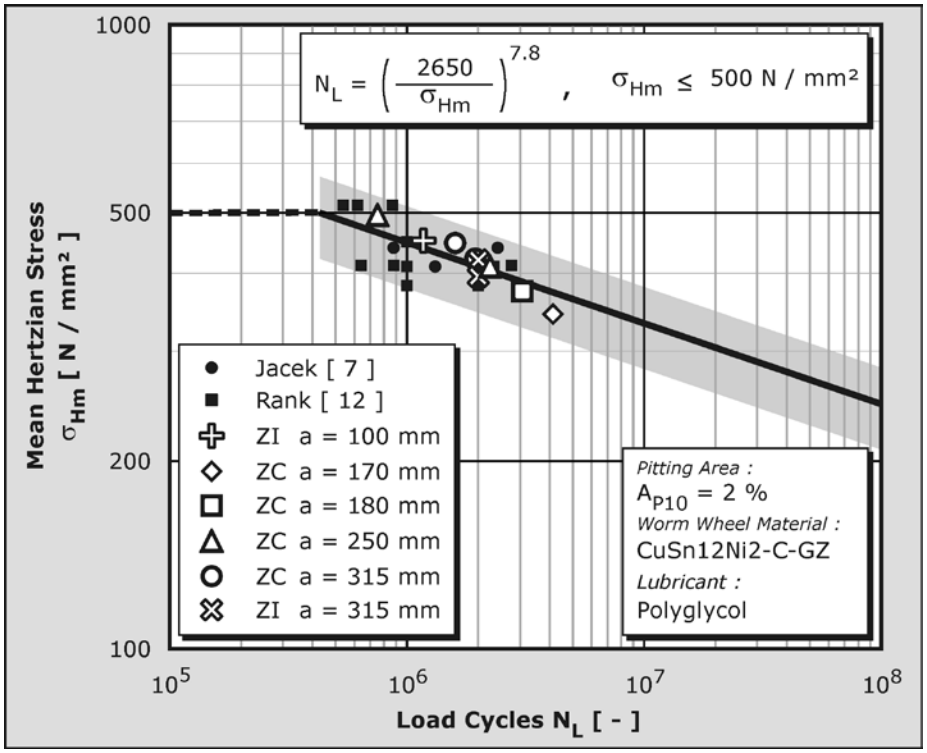

Figure 5 Part of Woehler diagram for end of pitting lifetime: Phase I.

References

1. Böhmer, T. "Entwicklung eines Standardtests für Schneckengetriebe zur Erprobung von Schmier- und Werkstoffen," Dissertation, Ruhr-Universität Bochum, 1991.
2. Bouché, B. "Reibungszahlen von Schneckengetrieben im Mischreibungsgebiet," Dissertation, Ruhr-Universität Bochum, 1991.
3. DIN 3974. "Toleranzen für Schneckengetriebeverzahnungen," Beuth Verlag, 1995.
4. DIN 3996. "Tragfähigkeit von Zylinder-Schneckengetrieben mit Achswinkel Σ = 90°," Beuth Verlag, 1998.
5. Hermes, J. "Tragfähigkeit von Schneckengetrieben bei Anfahrvorgängen sowie Lastund Drehzahlkollektiven," Dissertation, Ruhr-Universität Bochum, 2008.
6. Hohn, B. R. et al. "Grübchentragfähigkeit von Schneckengetrieben," Antriebstechnik 40 No. 12, 2001.
7. Jacek, A. "Werkstoff- und Fertigungsoptimierung für Schneckenräder," Dissertation, Ruhr-Universität Bochum, 2001.
8. Lutz, M. "Methoden zur rechnerischen Ermittlung und Optimierung von Tragbildern an Schneckengetrieben," Dissertation, TU München, 2000.
9. Niemann, G. and H. Winter. "Maschinenelemente" Band 3, Berlin Heidelberg, New York, Springer Verlag, 2, Auflage, 1986.
10. Octrue, M. "A New Method of Designing Worm Gears," ***Gear Technology*** **(*July/August*),** 1989, pp. 20–42.
11. Predki, W. "Hertz'sche Drücke, Schmierspalthöhen und Wirkungsgrade von Schneckengetrieben," Dissertation, Ruhr-Universität Bochum, 1982.
12. Rank, B. "Untersuchungen zur Grübchenbildung bei Zylinder-Schneckengetrieben," Dissertation, TU München, 1996.
13. Sievers, B. "Entwicklung von Programmroutinen zur Analyse von Tragbildern beliebiger Lage und Größe bei Schneckengetrieben," Diplomarbeit, Ruhr-Universität Bochum, 2007
14. Vill, D. "Schneckenverzahnungsprogramm," Frankfurt, Forschungsvereinigung Antriebstechnik e.V., Informationsblatt zum Vorhaben FVA 155/I, 1994.
15. Weisel, C. "Schneckengetriebe mit lokal begrenztem Tragbild," Dissertation, TU München, 2009.
16. Wilkesmann, H. "Berechnung von Schneckengetrieben mit unterschiedlichen Zahnprofilformen," Dissertation, TU München, 1974.

Prof. Dr.-Ing. K. Stahl studied mechanical engineering at the Technische Universitaet Muenchen before serving as research associate at the Gear Research Centre (FZG) at the Technical University Munich 1994 until 2000. In 2001 he received his PhD in mechanical engineering and that year started as gear development engineer at the BMW group in Dingolfing, subsequently being named head of "Prototyping, Gear Technology & Methods" in 2003. From 2006–2009 he changed to the BMW/MINI plant in Oxford, UK, first as group leader, and in 2007 as department leader for Validation Driving Dynamics and Powetrain. In 2009 Stahl returned to Munich, responsible for predevelopment and innovation management within BMW Driving Dynamics and Powertrain. Stahl was then named head in 2011 of the Institute for Machine Elements and the Gear Research Centre (FZG) at the Technische Universitaet Muenchen.

Prof. Dr.-Ing. B.-R. Höhn studied mechanical engineering at the Technical University Darmstadt (1965-1970) and served as an assistant lecturer (1970-1973) at the Institute for Machine Elements and Gears at the Technical University Darmstadt prior to becoming an assistant professor at the university (1973-1979); in 1978, he received his Ph.D. (Dr. Ing.) in mechanical engineering. In early April, 1979 Höhn worked as a technical designer in the department for gear development of the Audi, and by 1982 was head of the department for gear research and design for the automaker. In 1986 Audi named Höhn department head for both gear research and testing of automotive transmissions, until his departure in 1989 to become head of both the Institute of Machine Elements at the Technical University and of the Gear Research Centre (FZG). Since 2011, he has served as director emeritus of the Institute. Höhn has also served as vice president for VDI for research and development, as well as leader of working groups 6 and 15 for ISO TC 60—calculation of gears.

Dr.-Ing. J. Hermes studied mechanical engineering at the Ruhr Universität in Bochum (1998-2003) and served as research associate at the Gear Research Centre (LMGK) at the Ruhr Universität Bochum (2003-2007). In 2007 he received his Ph.D. in mechanical engineering. Over the past 10 years he has dealt with theoretical and experimental investigations of worm gears. Hermes' core areas of expertise are numerical simulations of the manufacturing process and the contact pattern of gears. He is the leader of working group NA 060-34-14 "worm gears" for DIN.

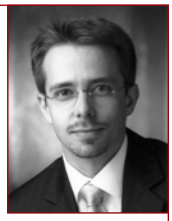

Dipl.-Ing. A. Monz has worked as scientific assistant at FZG in the field of worm gear drives until February, 2012. His core areas of expertise are tribology and load capacity of gears, both theoretical and experimental.